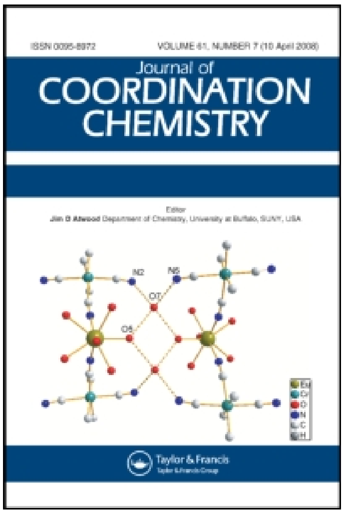

**Journal of Coordination Chemistry**
Publication details, including instructions for authors and subscription information:
http://www.informaworld.com/smpp/title~content=t713455674

# Synthesis, characterization and properties of polyaniline doped with transition metal substituted silicotungstate

Ronghua Ma[ab]; Fuping Wang[a]
[a] Department of Applied Chemistry, Harbin Institute of Technology University, Harbin 150080, China [b] College of Chemistry and Engineering, Qiqihar University, Qiqihar 161006, China

**To cite this Article** Ma, Ronghua and Wang, Fuping(2007) 'Synthesis, characterization and properties of polyaniline doped with transition metal substituted silicotungstate', Journal of Coordination Chemistry, 60: 22, 2421 — 2429
**To link to this Article: DOI:** 10.1080/00958970701272094
**URL:** http://dx.doi.org/10.1080/00958970701272094

*Journal of Coordination Chemistry*
Vol. 60, No. 22, 15 November 2007, 2421–2429

# Synthesis, characterization and properties of polyaniline doped with transition metal substituted silicotungstate

RONGHUA MA*†‡ and FUPING WANG†

†Department of Applied Chemistry, Harbin Institute of Technology University,
Harbin 150080, China
‡College of Chemistry and Engineering, Qiqihar University,
Qiqihar 161006, China

(*Received 19 June 2006; in final form 2 October 2006*)

Polyaniline hybrid material doped with transition metal mono-substituted silicotungstate $\beta_2$-$K_6[SiW_{11}M(H_2O)O_{39}]\cdot xH_2O$ ($M = Mn^{2+}$, $Co^{2+}$, $Cu^{2+}$, $Fe^{2+}$) were prepared for the first time. Their scanning electron microscopy (SEM), infrared (IR), UV–Vis, and X-ray diffraction (XRD) patterns confirm the existence of Keggin anions and form the space reticular structure. The material exhibits excellent proton conduction, its proton conductivity is $9\times10^{-2}\,\mathrm{s\,cm^{-1}}$ at room temperature (20°C).

*Keywords*: Polyaniline; Silicotungstate; Conductivity; Synthesis

## 1. Introduction

Heteropoly acids (HPA) are multifunctional materials and have been widely used in analytical and clinical chemistry, catalysis (including photocatalysis), biochemistry, medicine (antiviral, and even anti-HIV activity), and solid-state devices [1] owing to their unique combination of physical and chemical properties.

Inorganic–organic hybrid materials [2] have the advantages of organic materials such as light weight, flexibility, and good malleability and of inorganic materials such as high strength, heat stability, and chemical resistance [3]. Conducting organic polymers such as polyaniline (PANI) or polypyrrole (PPy) have attracted, on their own, great interest for their extraordinary properties and latent applications. These materials are formed by oxidative polymerization of the relevant monomers. The conducting state is usually obtained through *p*-doping, a course that takes place with the incorporation into the polymer of charge balancing anions. Therefore, aniline polymerizes in the presence of oxidizing agents and under acidic media to yield the protonated/oxidized form of emeraldine in its conducting state. In recent years, research on HPA in this field has been very active [4–6]. Physical-chemical properties of heteropoly complexes can be

---

*Corresponding author. Tel.: +86-452-2460178 (H); +86-452-2738223 (O). Email: mrh1963@163.com

*Journal of Coordination Chemistry*
ISSN 0095-8972 print/ISSN 1029-0389 online
DOI: 10.1080/00958970701272094

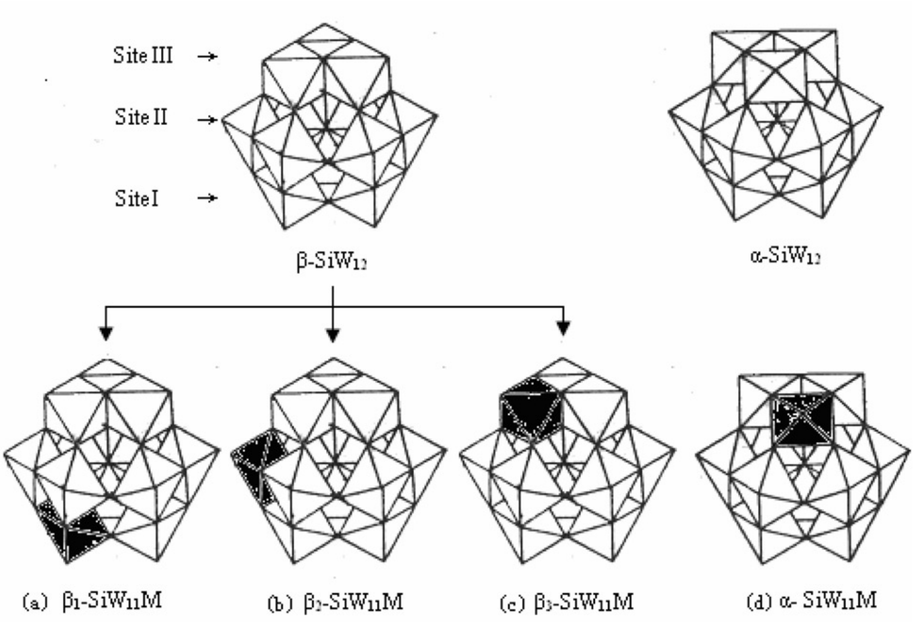

Figure 1. Idealized structures of Keggin anions; black is substituted atom occupational site.

modulated by changing their chemical environment by replacing some fragment atoms by transition metal atoms. The Keggin anion $\alpha$-$SiW_{12}O_{40}^{4-}$ ($\alpha$-$SiW_{12}$) is made of four $W_3O_{13}$ groups resulting from sharing of edges of strongly distorted $WO_6$ octahedra. These groups are associated around a central $SiO_4$ tetrahedron by sharing vertices. The polyanion thus has $T_d$ symmetry (figure 1). $\beta$-$SiW_{12}O_{40}^{4-}$ ($\beta$-$SiW_{12}$) derives from the Keggin structure by rotating a $W_3O_{13}$ group over $\pi/3$ around a threefold axis. The idealized polyanion thus has $C_{3v}$ symmetry (figure 1). As for $\beta$-$SiW_{12}O_{40}^{4-}$, there are three forms when the substituted atom in a mono-substituted $\beta$-$SiW_{12}O_{40}^{4-}$ is on different positions (figure 1): the substituted atom is in one of three sites of the rotated group (site III), a $\beta_3$-isomer (figure 1c); the substituted atom is adjacent to the rotated group (site II), a $\beta_2$-isomer (figure 1b); the substituted atom is far from the rotated group (site I), a $\beta_1$-isomer (figure 1a) [7]. In this article, we report for the first time the preparation of polyaniline doped with transition metal mono-substituted silicotungstate. Elemental analysis, IR, UV–Vis, SEM and XRD spectra characterized the polyaniline. The thermal stability and conductivity of the polyaniline doped with $\beta_2$-$K_6[SiW_{11}M(H_2O)O_{39}] \cdot xH_2O$ ($M = Mn^{2+}$, $Co^{2+}$, $Cu^{2+}$, $Fe^{2+}$) were studied.

## 2. Experimental

### 2.1. *Instrument and reagents*

All chemicals used were of analytical grade. The aniline used was distilled twice under vacuum. Leeman Lab ICP emission spectrometer, PE2400CHN element analyzer was used. FT–IR studies were carried out on Spectrum-One FT–IR spectrophotometer with

KBr pellets. The UV–Vis absorption spectra were obtained with a Tu-1901 UV spectrophotometer. XRD patterns were taken on a BD90 XJ 10-60N X-ray diffractometer with monochromated Cu Ka radiation. A FEISIRION scanning electron microscope (SEM) was employed to observe the morphology of the hybrid polyaniline/heteropoly acid material. TG measurements were carried out on SII Pryis Diamond thermal analyzer under a constant nitrogen flow, and scanning rate was 10.0°C min$^{-1}$. The conductivity was measured using a standard four-probe technique. Disk shape samples were prepared from powders using 20 MPa pressure at room temperature.

### 2.2. *Synthesis*

**2.2.1. $\beta_2$-$K_8[SiW_{11}(H_2O)O_{39}]\cdot 12H_2O$ (noted $\beta_2$-$SiW_{11}$).** Was synthesized according to [8] and examined by polarographic and IR spectra.

**2.2.2. $\beta_2$-$K_6[SiW_{11}M(H_2O)O_{39}]\cdot xH_2O$ (noted $\beta_2$-$SiW_{11}M$; M = $Mn^{2+}$, $Co^{2+}$, $Cu^{2+}$, $Fe^{2+}$).** Were prepared as follows: 6.4 g of $\beta_2$-$SiW_{11}$ was dissolved in 30 mL of water, the solution was maintained at 40°C, 4 mL of a 0.5 mol L$^{-1}$ solution of M(II) was added dropwise to the solution. The salt was precipitated with 2 g of potassium chloride, filtered and dissolved again in hot water. The potassium salt crystallized upon cooling. The potassium salt was examined by polarographic and IR spectra.

**2.2.3. Polyaniline doped with $\beta_2$-$SiW_{11}M$ (noted $\beta_2$-$SiW_{11}M$/PANI).** Freshly distilled aniline (2 mL) and acetic acid (1 mL) were placed in a mortar and cooled to −20°C for 20 min; then $\beta_2$-$SiW_{11}M$ (5 g) and $(NH_4)_2S_2O_8$ (3 g) were placed in the mortar, furbishing for ca 30 min. The color of solid changed to black–green, and was then washed with distilled water until pH = 7 was achieved, the powder was dried under vacuum at 50°C for 48 h. The results of elemental analysis are shown in table 1.

## 3. Results and discussion

### 3.1. *IR spectra*

The IR spectra of the materials are shown in figure 2. The intensity ratio of absorption at 1589 cm$^{-1}$ from the quinoid ring and at 1490 cm$^{-1}$ corresponding to benzene ring is more than 1 in IR spectra of the polyaniline base; bands in the range of 1200–1400 cm$^{-1}$ are C–N stretching band of an aromatic amine [9]. The characteristic band of polyaniline base is the N=Q=N stretch at 1166 cm$^{-1}$. The IR spectra change after

Table 1. Empirical formula and elemental analysis of materials (%).

| Empirical formula | W | C | H | N |
|---|---|---|---|---|
| $\beta_2$-$(C_6H_{4.5}N)(SiW_{11}Co)_{0.1003}$ | 52.53 | 18.72 | 1.20 | 3.64 |
| $\beta_2$-$(C_6H_{4.5}N)(SiW_{11}Mn)_{0.1011}$ | 52.15 | 18.68 | 1.19 | 3.68 |
| $\beta_2$-$(C_6H_{4.5}N)(SiW_{11}Cu)_{0.1008}$ | 53.08 | 18.74 | 1.26 | 3.66 |
| $\beta_2$-$(C_6H_{4.5}N)(SiW_{11}Fe)_{0.1009}$ | 53.05 | 18.75 | 1.21 | 3.65 |

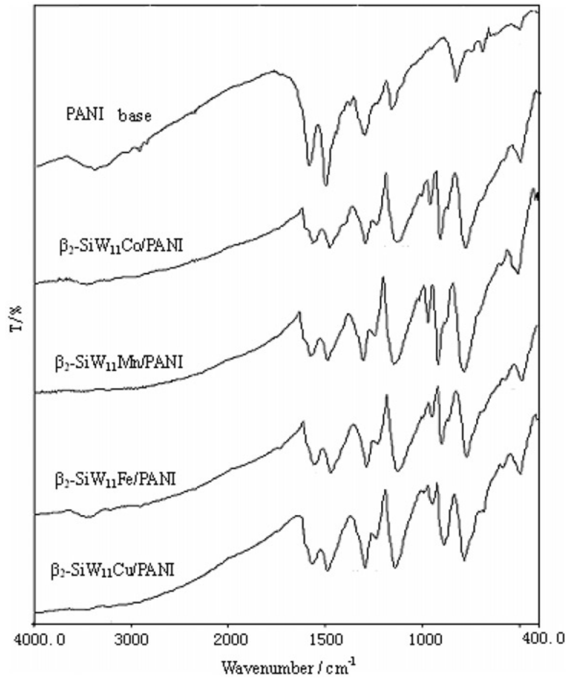

Figure 2. IR spectra of polyaniline doped with $\beta_2$-SiW$_{11}$M.

Table 2. IR spectra of polyaniline/SiW$_{11}$M (cm$^{-1}$).

| Samples | N=Q=N | N–B–N | C–N | Q–NH$^+$–B | W–O$_d$ | Si–O$_a$ | W–O$_b$–W | W–O$_c$–W |
|---|---|---|---|---|---|---|---|---|
| $\beta_2$-SiW$_{11}$Mn/PANI | 1573.98 | 1483.65 | 1302.91 | 1143.32 | 970.32 | 919.88 | 785.84 | 705.99 |
| $\beta_2$-SiW$_{11}$Fe/PANI | 1566.78 | 1483.93 | 1301.06 | 1142.50 | 965.26 | 916.88 | 789.90 | 698.61 |
| $\beta_2$-SiW$_{11}$Co/PANI | 1561.39 | 1484.20 | 1300.50 | 1142.17 | 968.08 | 918.51 | 790.79 | 650.06 |
| $\beta_2$-SiW$_{11}$Cu/PANI | 1574.79 | 1488.51 | 1302.83 | 1149.57 | 955.35 | 898.98 | 796.21 | 694.73 |
| PANI | 1589.16 | 1500.64 | 1303.37 | 1166.22 | | | | |

polyaniline is doped with transition metal substituted silicotungstate isomers: (1) 1589 cm$^{-1}$ band shifts slightly (ca 15–28 cm$^{-1}$) to lower frequency, 1490 cm$^{-1}$ band is unaffected and the relative intensity ratio of 1589/1490 cm$^{-1}$ decreases. This indicates that doping occurs in –N=, the benzene ring increases and the quinonoid ring decreases; (2) the band at ca 1142 cm$^{-1}$, characteristic of the protonated states [10], shows that the polyaniline molecule has been protonated; (3) bands in the range 700–1100 cm$^{-1}$, characteristic vibrations of the heteropoly acid appear [11], indicating that heteropoly acid has gone into polyaniline. The IR frequencies including assignments of the polyaniline are listed in table 2.

### 3.2. *UV–Vis spectra*

Figure 3 shows the UV–Vis absorption spectra of the intrinsic polyaniline and polyaniline doped with $\beta_2$-SiW$_{11}$M. For the intrinsic polyaniline, the band at

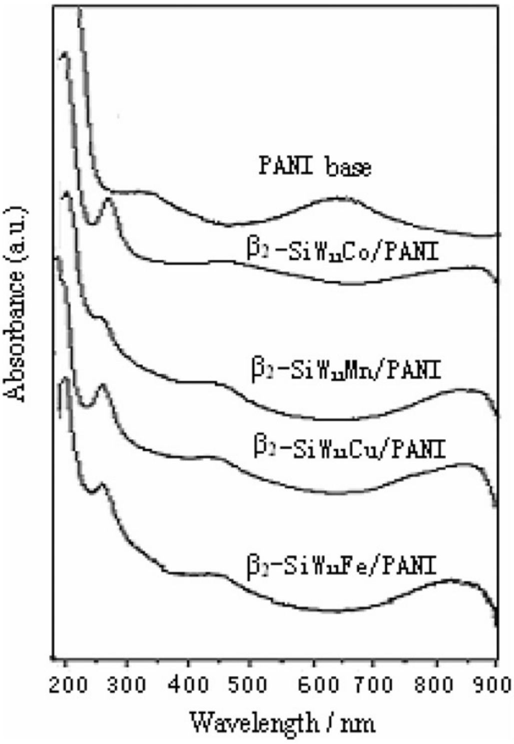

Figure 3. UV–Vis spectra of PANI doped with $\beta_2$-SiW$_{11}$M.

Table 3. Data of UV spectra of polyaniline/SiW$_{11}$M.

| Samples | $O_d \rightarrow W$ | $O_b/O_c \rightarrow W$ | The polaron absorption |
|---|---|---|---|
| $\beta_2$-SiW$_{11}$Co/PANI | 191 | 262 | 430, 845 |
| $\beta_2$-SiW$_{11}$Cu/PANI | 193 | 266 | 453, 854 |
| $\beta_2$-SiW$_{11}$Mn/PANI | 196 | 258 | 446, 851 |
| $\beta_2$-SiW$_{11}$Fe/PANI | 197 | 263 | 455, 840 |
| $\beta_2$-SiW$_{11}$Co | 193 | 251 | |
| $\beta_2$-SiW$_{11}$Cu | 196 | 259 | |
| $\beta_2$-SiW$_{11}$Mn | 200 | 253 | |
| $\beta_2$-SiW$_{11}$Fe | 197 | 255 | |

630 nm can be attributed to $\pi_b$–$\pi^*_q$ electronic transition of quinone and benzene units [12]. In the polyaniline doped with $\beta_2$-SiW$_{11}$M, two new bands at 450 and 850 nm appear, characteristic absorptions of the doped states of polyaniline, attributed to the polaron absorption [13]. The appearance of the polaron absorption band at 450 and 850 nm implies that the PANI has been doped, and that its conductivity is increased. Moreover, two stronger bands at about 190 nm and 260 nm appear in UV of polyaniline doped with $\beta_2$-SiW$_{11}$M; the band at 260 nm is characteristic of heteropoly acid, attributed to charge transfer of $O_b/O_c \rightarrow W$ [14]. The UV–Vis absorption spectra data of polyaniline doped with $\beta_2$-SiW$_{11}$M are listed in table 3.

### 3.3. *XRD spectra*

The X-ray diffraction pattern of the intrinsic polyaniline, $\beta_2$-SiW$_{11}$Co and polyaniline doped with $\beta_2$-SiW$_{11}$Co are shown in figure 4. The peaks of polyaniline doped with $\beta_2$-SiW$_{11}$Co differ from polyaniline base and heteropoly acid. No peak from crystalline form of heteropoly acid can be observed, indicating that HPA are inserted into the polymer matrix. The XRD pattern (figure 4) shows that the HPA in hybrid materials is amorphous; the most intense peak exists at about 7.8°.

### 3.4. *Scanning electron microscopy (SEM)*

Figure 5 shows a SEM photograph showing the microporous nature of this material and implies that polyaniline with heteropoly acid anion form a reticular sheet structure. We conclude that the heteropoly acid anion is incorporated in the bulk of the hybrid material.

### 3.5. *Thermal behavior studies*

The temperature of the exothermic peak of the DTA curves represents the sign of their thermostability. Figure 6 is the thermogram of polyaniline base. TG curve shows that there are two steps of mass loss: the weight loss at about 103.2°C is the loss of surface water and the weight loss at about 241°C is the beginning of degradation of polyaniline. Figure 7 shows the thermogravimetric measurements in a nitrogen atmosphere of polyaniline doped with $\beta_2$-SiW$_{11}$Co. The DTG curve of polyaniline doped with $\beta_2$-SiW$_{11}$Co with three peaks shows that $\beta_2$-SiW$_{11}$Co/PANI underwent three-stages of weight loss. From its TG curve, the first stage occurs in the range of 27.6–96.7°C with 7.19% mass loss from loss of surface water. The second stage occurs in the range of 375.3–500.0°C with 14.76% mass loss. This is the beginning of degradation of polyaniline, because the IR spectra at 375°C is stable (see figure 8b). In the DTA curve

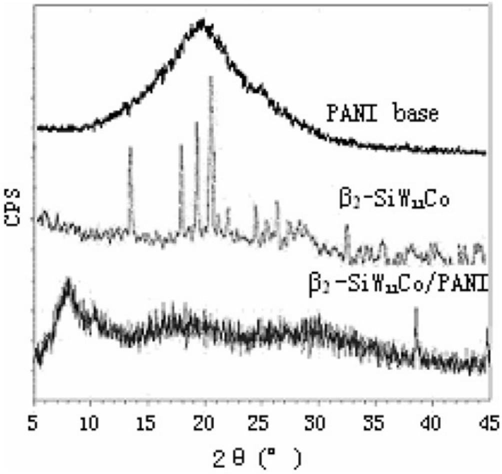

Figure 4. XRD patterns of different samples.

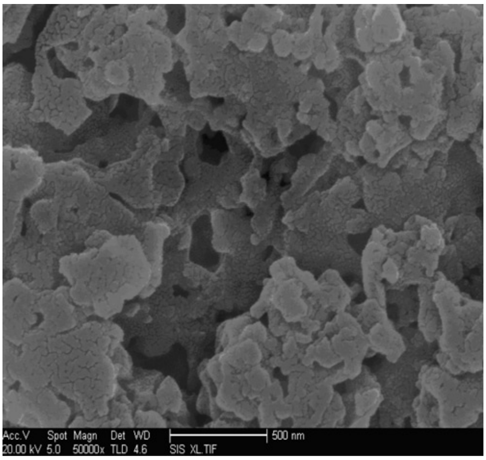

Figure 5. SEM of hybrid polyaniline by heteropoly acid.

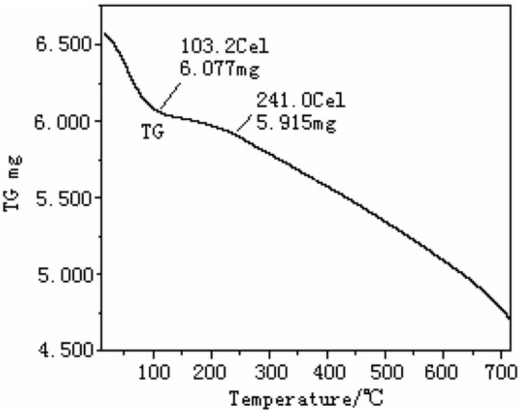

Figure 6. Thermogram of polyaniline base.

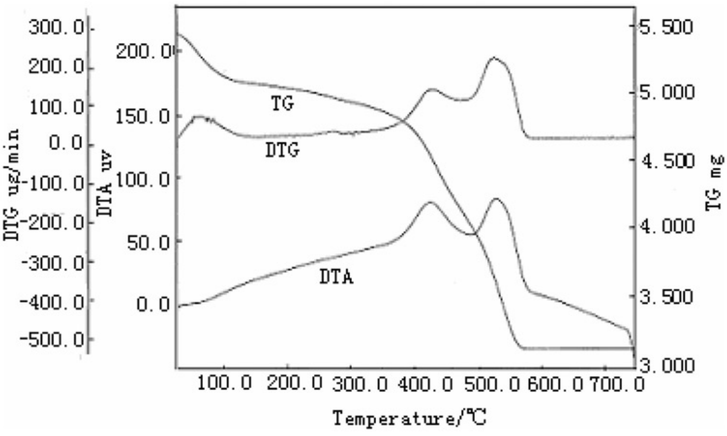

Figure 7. Thermogram of polyaniline doped with $\beta_2$-SiW$_{11}$Co.

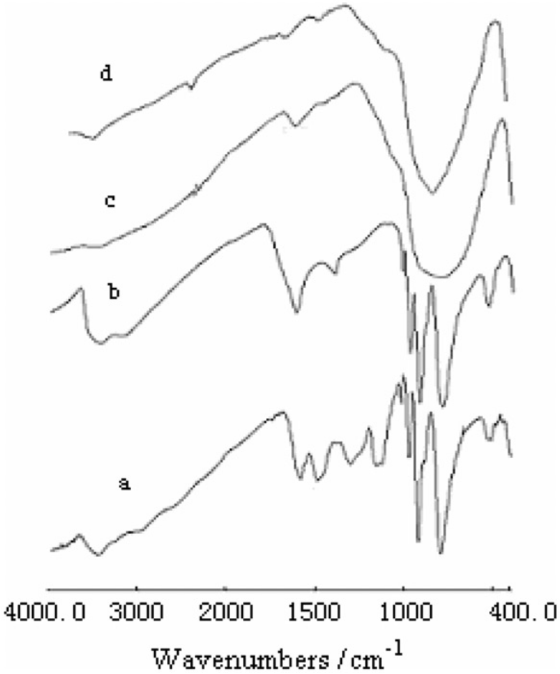

Figure 8. IR spectra of PANI material, treated by heating at (a) 120°C, (b) 375°C, (c) 500°C and (d) 600°C.

there is an exothermic peak at 434.8°C. The third stage occurs in the range of 500.0–572.5°C with 16.11% mass loss, due to degradation of polyaniline backbone and heteropoly acid backbone as indicated by the IR spectrum of the polyaniline, heated at 500°C for 60 min (figure 8c). In its DTA curve there is an exothermic peak at 530.3°C. Thermal analysis indicated that the thermal stability of polyaniline doped with $\beta_2$-SiW$_{11}$Co was higher than that of polyaniline base. Its decomposition temperature is about 134°C higher than that of polyaniline base showing that when polyaniline is doped by transition metal substituted silicotungstate, the thermostability increases.

### 3.6. *Conductivity*

Polyaniline base is insulating with conductivity of the order of $10^{-12}$ s cm$^{-1}$ [15]; protonation gives rise to an increase of electronic conductivity several orders of magnitude. Here the conductivity of all materials at room temperature is $\beta_2$-SiW$_{11}$Co/PANI: $9 \times 10^{-2}$ s cm$^{-1}$, $\beta_2$-SiW$_{11}$Fe/PANI: $6.3 \times 10^{-2}$ s cm$^{-1}$, $\beta_2$-SiW$_{11}$Mn/PANI: $3.6 \times 10^{-2}$ s cm$^{-1}$ and $\beta_2$-SiW$_{11}$Cu/PANI: $1 \times 10^{-2}$ s cm$^{-1}$. Comparing with conductivity of polyaniline doped with $H_3PMo_{12}O_{40}$ and $H_4PMo_{11}VO_{40}$, conductivity of polyaniline doped with $\beta_2$-SiW$_{11}$M is higher than that of polyaniline doped with $H_3PMo_{12}O_{40}$ and $H_4PMo_{11}VO_{40}$ ($H_4PMo_{11}VO_{40}$/PANI: $4.78 \times 10^{-4}$ s cm$^{-1}$; $H_3PMo_{12}O_{40}$/PANI: $1.34 \times 10^{-2}$ s cm$^{-1}$ [16]). This result indicates that the conductivity of polyaniline doped with transition metal substituted silicotungstate is higher than of polyaniline doped molybdenum-containing heteropolyacid.

## 4. Conclusion

We synthesized four polyaniline doped with transition metal substituted silicotungstate samples by using solid-state synthesis. The SEM, IR and XRD patterns confirm the existence of Keggin anions forming the space reticular sheet structure. The material exhibits excellent proton conduction, $9 \times 10^{-2}\,\mathrm{s\,cm^{-1}}$at room temperature (20°C). The thermal stability of polyaniline doped with $\beta_2$-$SiW_{11}Co$ was higher than that of polyaniline base.

## Acknowledgements

The financial support from the Science Foundation of the Heilongjiang Provincial Education Department for this work is greatly appreciated.

## References

[1] N. Giordano, P. Staiti, S. Hocevar, A.S. Arico. *Electrochim. Acta Commun.*, **41**, 397 (1999).
[2] G. Alberti, M. Casciola. *Solid State Ion.*, **145**, 3 (2001).
[3] Q.Y. Wu, G.Y. Meng. *Solid State Ion.*, **136**, 273 (2000).
[4] Y.L. Cui, J.W. Mao. *Mater. Chem. Phys.*, **85**, 416 (2004).
[5] J. Gong, X.J. Cui, Z.W. Xie, S.G. Wang, L.Y. Qu. *Synth. Met.*, **129**, 187 (2002).
[6] J. Gong, X.D. Li, B. Ding, D.R. Lee, H.Y. Kim. *J. Appl. Polym. Sci.*, **89**, 1573 (2003).
[7] A. Té, G. Hervé. *J. Inorg. Nucl. Chem.*, **39**, 2151 (1977).
[8] A. Té, G. Hervé. *J. Inorg. Nucl. Chem*, **39**, 999 (1977).
[9] L.X. Wang, F.S. Wang. *Acta Polymer. Sini.*, **3**, 264 (1989).
[10] L.Y. Qu, R.Q. Lu, J. Peng, Y.G. Chen, Z.M. Dai. *Synth. Met.*, **84**, 135 (1997).
[11] L.Y. Qu, Q.J. Shan, J. Gong, R.Q. Lu, D.R. Wang. *J. Chem. Soc., Dalton Trans.*, 4525 (1997).
[12] J.M. Wilbur, T.C. Sandreczki, I.M. Brown, D.J. Leopold, S. Mohite. *Synth. Met.*, **82**, 175 (1996).
[13] W.S. Huang, A.G. MacDiarmid. *Polymer*, **34**, 1833 (1993).
[14] J. Gong, Y.G. Chen, L.Y. Qu, Q. Liu. *Polyhedron*, **15**, 2273 (1996).
[15] M. Hasik, W. Turek, E. Stochmal, M. Lapkowski. *A. Pron, J. Catal.*, **147**, 544 (1994).
[16] S.G. Wang, H. Hong, J.X. Cui, J. Gong, L.Y. Qu. *Acta Chim. Cin*, **8**, 1166 (2001).